Ultra-High Accuracy Measurement of the Coefficient of Thermal Expansion for Ultra-Low Expansion Materials

Vivek G. Badami[*a], Michael Linder[b]
[a]Corning Tropel, Fairport, NY 14450; [b]Corning Inc., Corning, NY 14831

ABSTRACT

Microlithographic systems rely on precision alignment and a high-level of dimensional stability to meet their performance requirements. In critical applications, immunity to thermally induced dimensional changes is achieved by the use of ultra-low linear coefficient of thermal expansion (hereafter referred to as CTE and denoted by α) materials such as ULE® in components such as reflective optics and machine structures. The CTE of ULE® may be varied within limits during manufacture and is typically in the 0 ± 30 ppb K^{-1} range. A high-accuracy determination of the CTE is essential for both process control and for providing an essential input to the design of such systems for error budgeting purposes. Currently, there is a need for CTE determination with an expanded uncertainty $U(\alpha)$(k=2) <1 ppb K^{-1} in the 273-373 K (0-100°C) temperature range.

A survey of the state-of-the-art of high-accuracy absolute measurement of CTE is presented along with a discussion of the significant error sources in each of the current techniques. Metrology techniques, sample design and instrumentation are described along with uncertainty estimates for representative instruments. The design philosophy and prospects for a new instrument that satisfies the above mentioned need are described.

Keywords: Coefficient of thermal expansion, dilatometry, dilatometer, laser interferometry, ultra-high accuracy, uncertainty estimate, ULE, periodic nonlinearity

1. UNCERTAINTY ANALYSIS

The coefficient of thermal expansion (CTE) is defined as the fractional change in length per unit change in temperature.[1] Measurements of the CTE are typically realized by measuring the change in dimension and the accompanying change in temperature. Thus, given two measurements of the linear dimension of a sample, L_1 and L_2 made at temperatures T_1 and T_2, the *mean* CTE, α_m, over the temperature range $T_2 - T_1$ is given by

$$\alpha_m = \frac{L_2 - L_1}{L}\frac{1}{T_2 - T_1} = \frac{1}{\Delta T}\left[\frac{\Delta L}{L}\right] \tag{1.1}$$

where

L = length of sample at a given reference temperature

ΔT = change in temperature of sample

ΔL = change in length of sample corresponding to change in temp. of ΔT

The dimensionless quantity $\Delta L/L$ is referred to as the *dilatation* (or *dilation*). The expression for the CTE given by Equation 1.1 represents the mean or average CTE and is valid for relatively small dilatation. This expression for the CTE differs from the exact expression for the CTE which is given by

$$\alpha(T) = \frac{1}{dT}\left[\frac{dL(T)}{L(T)}\right]_T \tag{1.2}$$

Equation 1.2 is based on the slope of the length change vs. temperature curve at a single temperature and is the limiting case of Equation 1.1. The exact method of calculation should be specified as the results obtained from the two

[*] Contact: badamivg@corning.com; Phone (585) 388-3500; Fax: (585) 377-6332; http://www.tropel.com; Corning Tropel, 60 O'Connor Road, Fairport, NY 14450, USA.

expressions may differ significantly depending on the material and the experimental conditions used to make the measurement. In addition, there exist other definitions for the CTE which differ in subtle ways[2] and care must be taken to specify the correct definition.

The standard uncertainty in the CTE $u_c(\alpha)$ may be derived from uncertainty estimates of the various input quantities. This relationship is given by the Law of Propagation of Uncertainty[3] which is given by

$$u_c^2(y) = \sum_{i=1}^{N} \left(\frac{\partial f}{\partial x_i} \right)^2 u^2(x_i) + 2 \sum_{i=1}^{N-1} \sum_{j=i+1}^{N} \frac{\partial f}{\partial x_i} \frac{\partial f}{\partial x_j} u(x_i, x_j)$$

where

$y = f(x_1, x_2, x_3 \ldots x_N)$

$u(x_i)$ is the uncertainty associated with x_i

$u(x_i, x_j)$ is the covariance of x_i and x_j (1.3)

Assuming that the measured quantities are independent, application of Equation 1.3 to Equation 1.1 results in an expression for the standard uncertainty in CTE, $u_c(\alpha)$, which is given by

$$u_c(\alpha) = \sqrt{\left(\frac{1}{L\Delta T} \right)^2 u^2(\Delta L) + \left(\frac{\alpha}{\Delta T} \right)^2 u^2(\Delta T) + \left(\frac{\alpha}{L} \right)^2 u^2(L)} \quad (1.4)$$

where $u(\Delta L)$, $u(\Delta T)$ and $u(L)$ represent the uncertainties associated with the measurement of ΔL, ΔT and L respectively. Alternately, Equation 1.4 may be cast into a dimensionless form to derive an expression for the fractional uncertainty in CTE which is given by

$$\left(\frac{u_c(\alpha)}{\alpha} \right)^2 = \left(\frac{u(\Delta L)}{\Delta L} \right)^2 + \left(\frac{u(\Delta T)}{\Delta T} \right)^2 + \left(\frac{u(L)}{L} \right)^2 \quad (1.5)$$

The contributions of each of the sources of uncertainty in a practical measurement, i.e., for reasonable values of $u(\Delta L)$, $u(\Delta T)$ and $u(L)$ and for L = 100 mm, α = 10 ppb K^{-1} and ΔT = 10K are given in Table 1.

Table 1 Relative contributions of the various sources of uncertainty

Source	Example Value	Sensitivity Coefficient	Contribution (ppb K^{-1})
$u(\Delta L)$	0.5 nm	$\frac{1}{L\Delta T}$	0.5
$u(\Delta T)$	0.2 K	$\frac{\alpha}{\Delta T}$	0.2
$u(L)$	10 μm	$\frac{\alpha}{L}$	0.001
Standard uncertainty in CTE $u_c(\alpha)$			~0.53

From the above table it is evident that the dominant source of uncertainty in the measurement is the uncertainty associated with the measurement of the length change $u(\Delta L)$. The remaining uncertainties are far smaller contributors with the measurement being extremely insensitive to $u(L)$. Further, analysis of the sensitivity coefficients shows that the influence of $u(\Delta T)$and $u(L)$ scales directly with the CTE while the sensitivity to $u(\Delta L)$ is independent of the CTE. The sensitivity to $u(\Delta L)$ may be reduced by increasing the size of the temperature step ΔT and/or the length of the sample L. The size of the temperature step is a trade-off between a reduction in uncertainty associated with a large ΔT and the increase in the error due to the difference between the true value of the CTE (Equation 1.2) and the mean value obtained

over the interval ΔT (Equation 1.1). In other words, a smaller ΔT results in more data points in a given interval resulting in a 'smoother' curve at the expense of increased uncertainty for each data point.

Based on the foregoing analysis, it is evident that the dominant contributor to the uncertainty of the measurement is the uncertainty in the dilatation ($\Delta L/L$) of ≈ 5 parts in 10^9. This implies $u(\Delta L)$ = 0.5 nm in a typical sample length of 100 mm.

2. GENERALIZED MEASUREMENT MODEL

The measurement of CTE may be described in terms of a generalized dilatometer system, a schematic of which is shown in Figure 1a. The key parts of such a system are shown in the schematic. The four main components are:

1. A means for sensing the ends of the sample. This is represented in the schematic by the anvil on one end and by the indicator contact on the other. In a dilatometer, this may take the form of mechanical contacts, light incident upon reflective end-faces, capacitance gages, etc.
2. A measurement system for detecting and measuring the change in length of the sample, represented here by the dial indicator. In a practical system, this may be implemented using a LVDT, laser interferometer, etc.
3. A structural system or frame that positions the above components relative to the sample and serves as a return path for the metrology loop (discussed below). This component is represented by the C-frame of the instrument in the schematic and is typically comprised of the instrument structure or a second measurement path in a real instrument.
4. A method for changing the temperature of the sample. This may take the form of a furnace/cooler that surrounds the sample.

The interaction of these components and the overall behavior of such an instrument may be understood in terms of the *metrology loop*. The metrology loop is a conceptual construct that takes the form of a closed loop that passes through all components of the system that define the length of the sample. It is shown in the schematic as a dashed line, which runs from one end of the sample through the end contact, the passive frame and measuring system and returns through the other end to close the loop. Changes in length along any part of this loop manifest themselves in the measurement as apparent changes in the length of the sample and are indistinguishable from the dimensional changes of the sample. Figure 1a shows the desired situation where the indicator measures only the expansion of the sample. In contrast, Figure 1b shows the more realistic situation where all components of the system deform thermally producing a measurement that is a convolution of these individual deformations.

The thermal deformation of the frame of the instrument often constitutes the largest source of uncertainty in the measurement. The challenge is to confine the temperature changes to the sample while isolating the rest of the metrology loop. In practice, thermal coupling between the energy source and the frame is an issue that can result in spurious displacements. The frame may take the form of a physical structure or an optical reference in an interferometer system. The stability of the frame is typically achieved by some combination of environmental control and/or usage of materials with significantly lower CTE (often several orders of magnitude smaller) than that of the sample such as ULE®, Zerodur® or Invar. However, for the measurement of ultra-low expansion materials, stringent environmental control of the frame is the only option, as a physical reference frame with a CTE significantly lower than the sample is no longer a viable choice.

In high-accuracy systems, the reference frame is replaced by an equivalent optical path. Changes in this optical path length are sensed as part of the overall measurement. Thus, the change in length of the reference frame is monitored as part of the measurement. Since optical path length is the product of refractive index and physical path length, changes in either are sensed as dimensional changes. In order to minimize the effects of changes in refractive index, such measurements are typically performed in vacuum, effectively producing a reference frame that is minimally affected by changes in the environment and is the equivalent of a frame with low CTE.

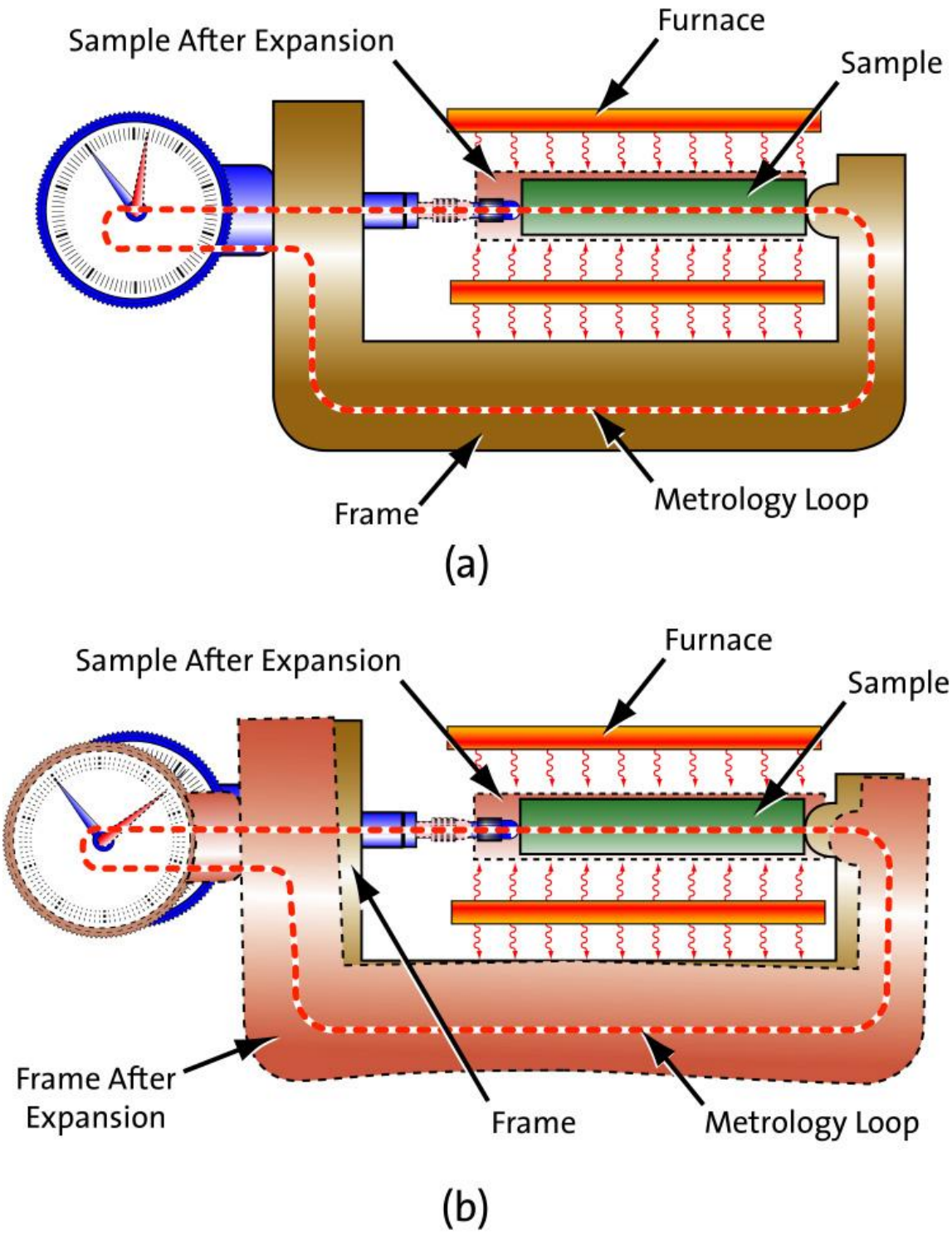

Figure 1 Generalized measurement model showing a) ideal situation b) actual measurement

3. MEASUREMENT TOPOLOGIES

This section discusses the common measurement topologies (configurations) used to perform high-accuracy dilatometric measurements. The classification is based on sample geometries rather than measurement techniques. Although there may be a multiplicity of measurement techniques for each sample configuration, the measurement techniques have many sources of uncertainty in common. A schematic representation of each technique is presented along with an example of a practical realization. This review confines itself to absolute high-accuracy interferometric techniques. A more general review of measurement techniques may be found in the paper by James *et al.*[2] Uncertainties associated with measurement of the length change are emphasized, as this is the dominant contributor to the overall uncertainty.

3.1 Single-sided measurement with sample and base plate

This configuration is represented schematically in Figure 2a and is the configuration of choice for a large number of instruments.[4-23] It consists of a sample which is attached to a base plate. Measurements are made directly off the front face of the sample (with an auxiliary mirror in some cases[19]) and indirectly off the rear face (via the base plate). The two dial indicators schematically show the differential nature of the measurement. This arrangement is designed to be immune to gross motions of the sample along the line of action of the indicators. Thus, in principle, the difference between the readings of the two dial indicators represents only the dimensional changes of the sample. The routing of the metrology loop indicates that any dimensional changes of the frame, i.e., any changes that result in a change in relative position between the indicators are interpreted as a dimensional change in the sample.

The two indicators may be replaced by a variety of measurement methods. However, for high-accuracy measurements, interferometers of different kinds are the method of choice. Practical realizations that use Michelson type interferometers,[4-6] Jamin interferometers,[7] multiple-wavelength interferometers[8-10] and Fizeau interferometers[11-15] can be found in the literature. While the exact implementation may vary, these implementations share a number of common characteristics including sources of uncertainty.

The discussion in the foregoing paragraphs serves as the basis for an analysis of uncertainty sources of an interferometer implementation of this configuration. This implementation is due to Bennett[17] and is shown in Figure 2b. This system is the basis for a number of similar systems.[18-23] The sample arrangement is symmetric with the two reference beams straddling the sample.

As noted in the previous section, any changes in the optical path length not directly related to thermally induced dimensional changes in the sample constitute sources of uncertainty. Examples of such interferometer related errors include:

- Environmental effects due to temperature, pressure, humidity and CO_2 concentration affect the results due to the path length mismatch in the two arms of the interferometer and due to temperature gradients. This is typically addressed by operating the system in vacuum or in an atmosphere of helium. Compensation based on pressure, temperature and humidity information is another somewhat less accurate option.
- A similar contribution may be observed due to temperature gradients in the glass as a result of unequal changes of the index with temperature
- Changes in the phase change on reflection with temperature at various coatings. In this configuration, these variations may be common-mode to the extent that the temperature is uniform in the system
- Stability of joints in the interferometer between the various optical components
- Errors in measurement of phase difference
- Frequency stability of the laser source
- Errors due to interferometer nonlinearity
- Variation in beam pointing

Examples of possible errors related to the sample include

- Variations in the joint between sample and base plate. The sample may be in simple mechanical contact under gravity (or spring force) loading or may be optically contacted. The measurement assumes that the joint is

stable over the measurement. Joint stability is directly reflected in the observed dimensional changes and constitutes a major source of uncertainty
- Coupling of sample translation perpendicular to the beam axis into the measurement due to non-parallelism of the reflecting faces
- Sample tilt (more pronounced effect in asymmetrical configurations[16])
- Expansion of coatings. In this configuration, these variations may be common-mode to the extent that the temperature is uniform in the system
- Variation in modulus of elasticity with temperature resulting in sample deflections with temperature
- Variation in acceleration due to gravity
- Sample and base plate bending due to temperature gradients/variations in CTE
- Deflections due to CTE mismatch between sample and base plate

This configuration has some major advantages
- A null test is easily performed by removing the sample and thus allowing measurement of the base plate alone
- Samples of various lengths may be accommodated easily. This feature is invaluable in the determination of systematic errors

Okaji *et al* quote a standard uncertainty of 16 ppb K^{-1} over the range of 6-273K and 9 ppb K^{-1} near room temperature.[19] Most of the uncertainty is attributed to uncertainty in length measurement caused by periodic errors in the heterodyne interferometer. This particular setup utilizes a second mirror that is optically contacted to the front face of the sample in addition to the baseplate. Okaji and Birch[22] also report agreement between results of measurements made on separate instruments at NRLM and NPL of fused silica to within 40 ppb K^{-1} for ΔT=30K. A good estimate of the levels of uncertainty associated with this type of sample configuration using a variety of different instruments may be obtained from the results of the EUROMET intercomparsion[24] which reports expanded uncertainties (k=2) of 5-60 ppb K^{-1}on the measurement of the CTE of a 100 mm Zerodur® gage block.

3.2 Double-ended measurement without auxiliary optics

This configuration is shown schematically in Figure 3a. The measurement is made on both ends of the sample. The two sensors are linked through the frame. The frame is included in the metrology loop and any changes in the frame dimensions are indistinguishable from changes in sample length.

Relatively few examples of a double-ended measurement are to be found in the literature.[25-27] An implementation that uses two Michelson interferometers that is due to Wolff & Eselun is shown in Figure 3b. This system is essentially a refinement of another system developed by one of the authors[25] and addresses some of the shortcomings of the earlier system. It consists of two separate Michelson interferometers with separate reference arms which are referenced to one another through an artifact made of ultra-low expansion material e.g., ULE®. This approach exploits the fact that for a given temperature change, the expansion scales with the length. Therefore, by reducing the length of the reference artifact, the absolute expansion of the artifact, and hence its uncertainty contribution, may be minimized. This method considerably shortens and stabilizes the metrology loop, which now passes through the artifact rather than the instrument frame.

Such a system shares many of the sources of uncertainty with the system described in the previous section. The significant differences are

- Uncertainties due to the optical contact are eliminated.
- Sample preparation is simpler than in the previous case.
- In instrument configurations where the metrology frame passes through the instrument frame, the stability of the instrument frame is a significant contributor to the instrument uncertainty.[25] In the particular configuration described here, the contributions of the instrument frame are minimized by use of a reference artifact.
- Spatially separated reference and measurement arms result in susceptibility to optical path length changes due to environmental effects, i.e., changes due to variation in refractive index.
- Null test to determine instrument stability is difficult to perform in some instrument configurations.[25]

As in the previous configuration, samples of different lengths may be accommodated for determination of systematic errors. Wolff *et al* report a noise-limited uncertainty of 20 ppb K^{-1} for a temperature step of 4K using a 100 mm sample. This corresponds to an uncertainty of 8 ppb K^{-1} for a 10K step and is based on a statistical evaluation of noise and measurement repeatability and does not include any systematic errors.[26]

3.3 Double-ended measurement with auxiliary optics

This configuration is diagrammed schematically in Figure 4a and represents an inversion of the previous configuration. As in other configurations, dimensional changes in the frame are indistinguishable from changes of the sample.

This type of measurement is performed by constructing a high-finesse Fabry-Perot etalon with the sample as the spacer[29-31] as shown in Figure 4b. Mirrors with high-reflectance coatings are optically contacted to the ends of the sample. The cavity is probed with a laser whose frequency is locked to a transmission maximum of the cavity. The frequency of the probe laser is determined by beating it against a frequency standard. The change in resonance frequency of the etalon is a measure of the change in optical path length. This method of displacement measurement has extremely high sensitivity compared to the previous methods (capable of sensing dilatation ~10^{-11}).[31] Further, there is no separate reference arm as in the method described in Sections 3.1 and 3.2. Ideally, the observed path length change is caused solely by dimensional changes of the spacer. In practice, any effect that produces an optical path length change contributes to the observed displacement.

This configuration differs from the foregoing configurations in many ways and has some sources of uncertainty that are unique to it. The significant differences include:

- Uncertainty due to the behavior of the optical contacts. This contribution is greater than that of the configuration with one optical contact (Section 3.1). Optical contacting results in the build-up of stresses at the interface as a result of the contacting process. This situation may be further exacerbated by differences in CTE between the spacer and the mirrors. Berthold[30] reports a strain rate of 1.6 $\times 10^{-10}$/day for an *average* optical contact. This corresponds to approximately 4 pm over a typical six hour period required to change the temperature of the sample. While this is a negligible source of uncertainty as reported, the variability associated with the optical contacting process and the consequent uncertainty contribution remain an issue. Further, this value was obtained under conditions of constant temperature. To the authors knowledge no experimental data exists that quantifies the behavior of the contact as a function of temperature.
- Temperature dependent changes in the phase change upon reflection of the high-reflectance coatings. Other effects may also be observed due to changes in the coating, e.g., due to adsorbed water films when the sample is put into a vacuum.[31]
- Changes in the refractive index with temperature. This type of measurement is usually made *in vacuo* to minimize these effects. Even so, careful control of the vacuum environment is required to avoid significant contributions.
- Uncertainty in phase measurement is replaced by the uncertainty in frequency measurement. This includes the frequency resolution.
- The system is not as sensitive to sample alignment relative to the laser beam. Further, the output signal may be used to realign the sample.
- Sample preparation is considerably more complex than in the previous configurations.
- Null test can be performed relatively easily.

The greatest unknown in this technique is the behavior of the optical contacts and the high-reflectance coatings. Attempts have been made to quantify these effects by measuring etalons of different lengths.[30] However, data from such an experiment are valid only to the extent that the systematic effects are reproduced between the two etalons. A bounding value for the contribution of the change in phase change on reflection with temperature of 6 ppb K^{-1} has been suggested by one investigator[28] based on discrepancies between the results of measurement made by Jacobs and Corning Glass Works on ULE 7971 by a dissimilar method.[29] While this technique exhibits a precision < 1 ppb K^{-1}, based on round-robin studies, the overall uncertainty of this technique is estimated to be ~5 ppb K^{-1}.

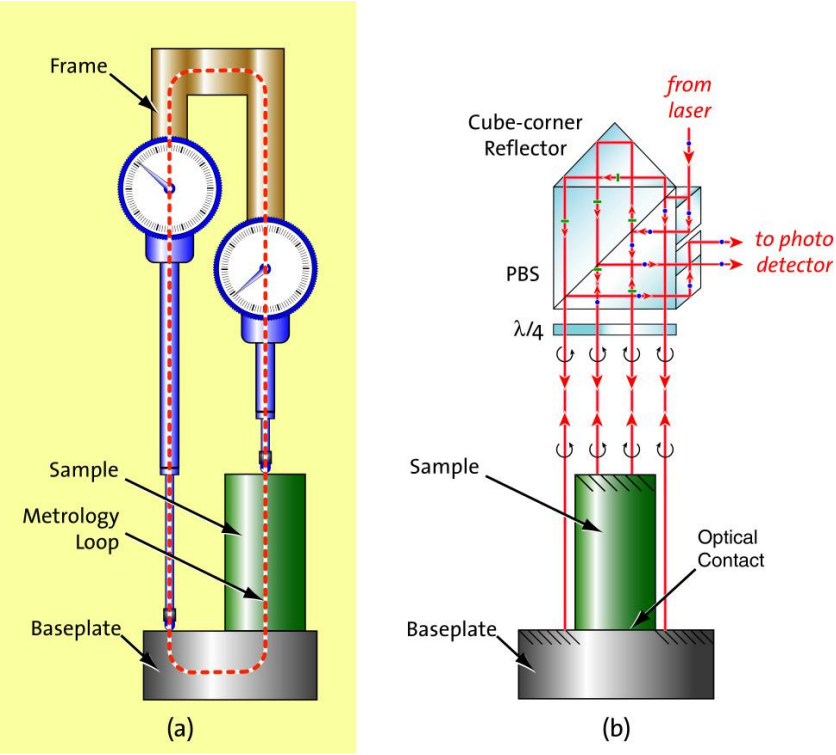

Figure 2 Sample/baseplate single-sided measurement a) Schematic b) Modified Michelson implementation

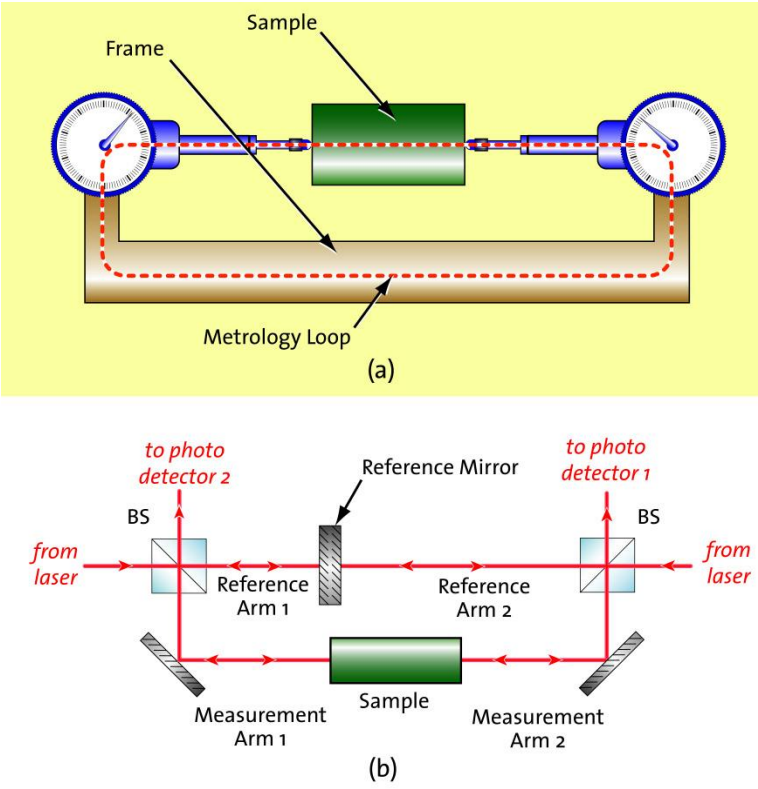

Figure 3 Double-ended measurement without auxiliary optics a) Schematic b) Double Michelson implementation

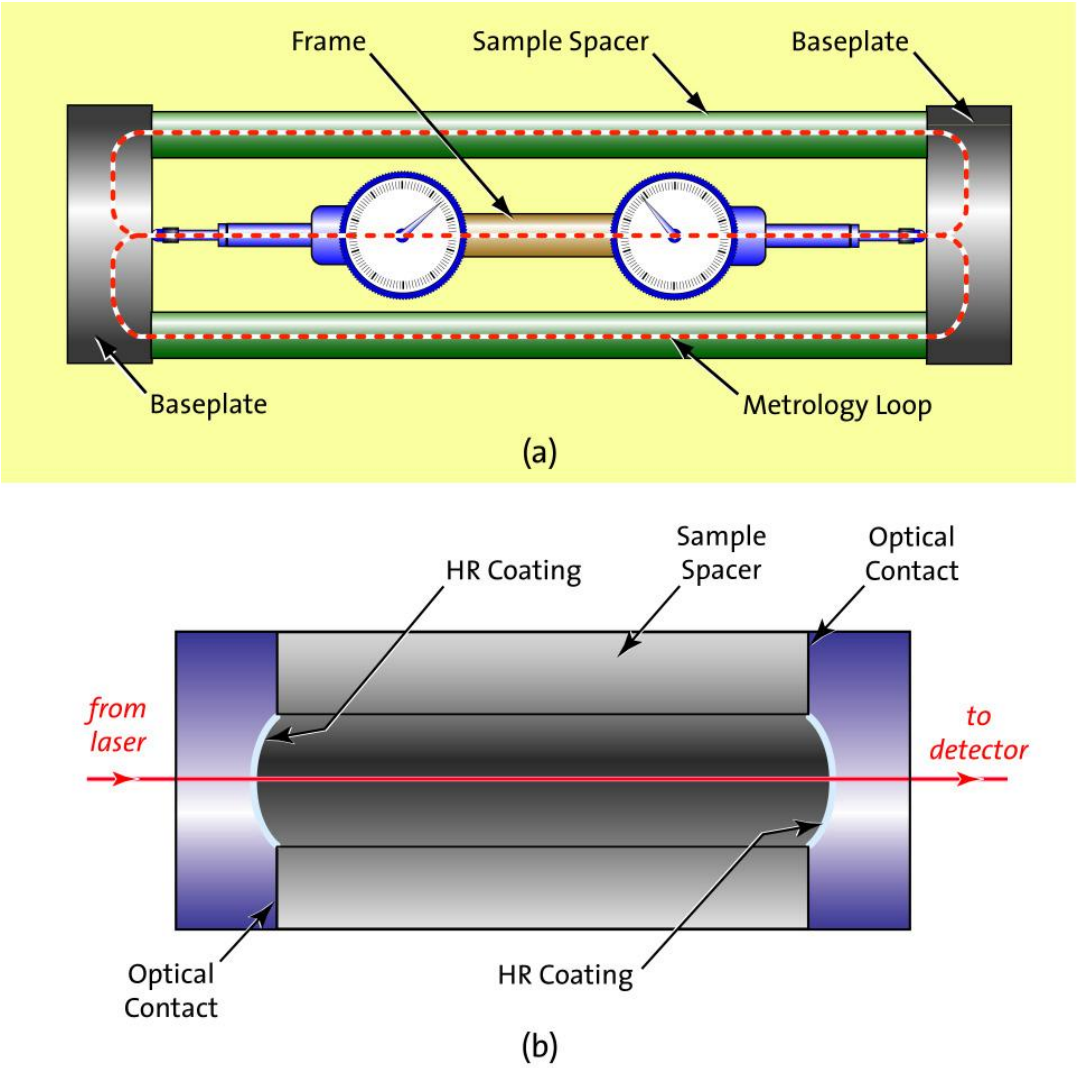

Figure 4 Double-ended measurement with auxiliary optics a) Schematic b) Fabry-Perot implementation

4. CONCLUSIONS

From the foregoing discussion it is evident that there exist several techniques that can perform measurements of the CTE of low-expansion materials with uncertainties in the ~5-60 ppb K^{-1} range. The current requirement represents an improvement of at least a factor of five. Based on the discussion of uncertainty sources, a set of characteristics for an instrument designed to meet the required uncertainty goal of 1 ppb K^{-1} are listed below:

a) A stable metrology loop which eliminates or minimizes the sources of spurious displacement
   i) Elimination of the uncertainty due to optical contacts or other joining methods. Such an improvement could result from a redesign of the sample geometry resulting in a monolithic sample or from a instrument configuration that does not require auxiliary optics or a combination of the two.
   ii) Elimination of the uncertainty due to the temperature dependent behavior of coatings. This could be achieved by elimination of coatings or by an instrument design that makes such changes common-mode and hence rejects their contribution.

iii) Balanced optical paths in vacuum as well as glass. In the case of separate reference arms (as in a Michelson interferometer), the two arms of the interferometer should have minimum spatial separation in order to make environmental effects common mode. Interferometer design to balance the paths within the optics also serve to mitigate errors due to optical path changes within the glass resulting from changes in temperature.

iv) Sample alignment stability and beam pointing stability. The alignment of the sample relative to the beam should be stable in order to prevent the probing of different parts of the sample by the beam. This results in contributions from imperfections in the sample geometry. Stable sample supports and active alignment systems are a possible solution.

b) Interferometer nonlinearity errors. A source of uncertainty that is often ignored is nonlinearity in the interferometer outptut due to beam-mixing.[32-35] This represents a very significant source of uncertainty at this level of accuracy and should be addressed in any system that uses an interferometer with a potential for beam mixing.

c) Systematic errors. Replacement of the reference frame with an equivalent optical path length only addresses a part of the metrology loop. Other sources of uncertainty such as the phase behavior of reflective optics, thermal influences on optical contacts and deformation of the optics used to generate the reference optical length can result in thermal effects that bias the measurement. Many of these effects are likely to be highly repeatable and for this reason do not adversely affect the repeatability of the measurement, making it insufficient to state an uncertainty based on the scatter in the results of multiple determinations. It is therefore important to consider the entire uncertainty budget (including systematic effects) when making an uncertainty statement. It is likely that recent developments in high-resolution/high-accuracy interferometry[37] which include techniques that eliminate periodic nonlinearities,[32-36] ultra-stable lasers[38] and high-resolution phase interpolators will reduce the uncertainty associated with measurement of the length change to well below 1 nm. At this point systematic errors are likely to dominate. Systematic errors are typically identified and quantified through round-robin type inter-comparisons.[24] This is likely to be challenging at the target level of uncertainty. Alternately, an experimental technique that is self-checking would be clearly superior. Okaji *et al*[19] and Berthold[30] have used measurements of samples of different lengths in order to identify systematic errors. Okaji estimates the bias of his system[19] by measuring the CTE of 10 mm and 20 mm samples cut from a single sample of SRM 739. Based on the assumption that the experiment is reproducible between the two measurements and the CTE for the two specimens is the same, he derives an instrument bias of 1.4 nm K^{-1}, which equates to a systematic error of 14 ppb K^{-1} in the 100 mm samples commonly used for CTE measurement. Such errors are considerably larger than the stated accuracy goal and are likely to dominate once the fringe determination errors of the interferometers systems are reduced to less than 1nm. Thus, an experimental setup that incorporates ways of identifying systematic errors and is self-checking is extremely desirable. One possible arrangement for identifying such errors is a setup that accommodates changes in sample length with minimum impact on the rest of the setup. Further, the sample design should allow for inter-comparison measurements with other instruments as another method for identifying systematic errors.

Meeting the goal for CTE measurements with a standard uncertainty < 0.5 ppb K^{-1} represents a significant challenge. Assuming a 100 mm sample and a 10 K temperature step (see Table 1), this implies a length measuring uncertainty of <0.05 nm K^{-1}. This is achievable with interferometric techniques and is clearly in the realm of absolute techniques since at the present time, in addition to other sources of uncertainty, there is no source for a reference sample with the requisite uncertainty for performing a relative measurement.

REFERENCES

1. American Society of Testing and Materials ASTM E 289, pp. 166-174, 1995.
2. J. D. James, J. A. Spittle, S. G. R. Brown and R. W. Evans, "A review of measurement techniques for the thermal expansion coefficient of metals and alloys at elevated temperatures," *Meas. Sci. Technol.*, **12**, pp. R1-R15, 2001.
3. Guide to the Expression of Uncertainty in Measurement, ISO, 1995.
4. W. Hou and R. Thalmann, "Thermal expansion measurement of gauge blocks," *Proc. SPIE Vol. 3477 Recent Developments in Optical Gauge Block Metrology*, pp. 272-278, 1998.

5. W. D. Drotning, "Laser interferometer for high temperature isothermal length changes over long time periods," *Rev. Sci. Instrum*., **52**(12), pp. 1896-1900, 1981.
6. R. B. Roberts, " Absolute dilatometry using a polarization interferometer: II," *J. Phys. E: Sci. Instrum.*, **14**, pp. 1386-1388, 1981.
7. T. S. Aurora, S. M. Day, V. King and D. O. Pederson, "High-temperature laser interferometer for thermal expansion and optical length measurements," *Rev. Sci. Instrum*., **55**(2), pp. 149-152, 1984.
8. A. Lewis, "Measurement of length, surface form and thermal expansion coefficient of length bars up to 1.5 m using multiple-wavelength phase-stepping interferometry," *Meas. Sci. Technol*., **5**, pp. 694-703, 1994.
9. H. Darnedde, "High-precision calibration of long gauge blocks using the vacuum wavelength comparator," *Metrologi*a, **29**, pp. 349-359, 1992.
10. R. Schödel and G. Bönsch, "Precise interferometric measurements at single crystal silicon yielding thermal expansion coefficients from 12 ºC to 28 ºC and compressibility," *Proc. SPIE Vol. 4401 Recent Developments in Traceable Dimensional Measurements*, pp. 54-62, 2001.
11. E. B. Hughes, "Measurement of the linear thermal expansion coefficient of gauge blocks by interferometry," *Proc. SPIE Vol. 2088 Laser Dimensional Metrology: Recent Advances for Industrial Application*, pp. 179-189, 1993.
12. G. E. Merritt, "Application of the interferometer to measurements of the thermal dilatation of ceramic materials," *Scientific Papers of the Bureau of Standards*, pp. 357-373, 1923.
13. T. A. Hahn, "Thermal Expansion of Copper from 20 to 800 K- Standard Reference Material 736," *J. Appl. Phys.*, **41**(13), pp. 5096-5101, 1970.
14. R. E. Edsinger and J. F. Schooley, "A High-Accuracy Dilatometer for the Range –20 to 700 ºC," *Int. J. Thermophysics*, **12**(4), pp. 665-677, 1991.
15. W. A. Plummer and H. E. Hagy, "Precision Thermal Expansion Measurements on Low Expansion Optical Materials," *Applied Optics*, **7**(5), pp. 825-831, 1968.
16. E. G. Wolff and S. A. Eselun, "Thermal expansion of a fused quartz tube in a dimensional test facility," *Rev. Sci. Instrum*., **50**(4), pp. 502-506, 1979.
17. S. J. Bennett, "An absolute interferometric dilatometer," *J. Phys. E: Sci. Instrum.*, **10**, pp. 525-530, 1977.
18. K. P. Birch, "An automatic absolute interferometric dilatometer," *J. Phys. E: Sci. Instrum.*, **20**, pp. 1387-1392, 1987.
19. M. Okaji, N. Yamada, K. Nara, H. Kato, "Laser interferometric dilatometer at low temperatures: application to fused silica SRM 739," *Cryogenics* **35**, pp. 887-891, 1995.
20. M. Okaji, H. Imai, "A practical measurement system for accurate determinations of linear thermal expansion coefficients." *J. Phys. E: Sci. Instrum*., **17**, pp. 669-673, 1984.
21. M. Okaji, H. Imai, "A high-temperature dilatometer using optical heterodyne interferometry," *J. Phys. E: Sci. Instrum.*, **20**, pp. 887-891, 1987.
22. M. Okaji, K.P. Birch, "Intercomparison of Interferometric Dilatometers at NRLM and NPL," *Metrologi*a, **28**, pp. 27-32, 1991.
23. M. Okaji, N. Yamada, H. Kato, K. Nara, "Measurements of linear thermal expansion coefficients of copper SRM 736 and some commercially available coppers in the temperature range 20-300 K by means of an absolute interferometric dilatometer," *Cryogenic*s, **37**(5), pp. 251-254, 1997.
24. R. Thalmann, "International Comparison Final Report," *Metrologi*a, **33**, pp. 187-188, 1996.
25. E. G. Wolff and S. A. Eselun, "Double Michelson Interferometer for Contactless Thermal Expansion Measurements," *Proc. SPIE Vol. 192 Interferometry*, pp. 204-208, 1979.
26. E. G. Wolff and R. C. Savedra, "Precision Interferometric Dilatometer," *Rev. Sci. Instrum.*, **56**(7), pp. 1313-1319, 1985.
27. A. P. Miller and A. Cezairliyan, "Interferometric Technique for the Subsecond Measurement of Thermal Expansion at High Temperatures: Applications to Refractory Metals," *Int. J. Thermophysics*, **12**(4), pp. 643-656, 1991.
28. S. R. Patterson, "Interferometric Measurement of the Dimensional Stability of Superinvar," UCRL-53787, University of California, pg. 22, 1988.
29. S. F. Jacobs, J. N. Bradford and J. W. Berthold III, "Ultraprecise Measurements of the Thermal Coefficients of Expansion," *Applied Optics*, **9**(11), pp. 2477-2480, 1970.
30. J. W. Berthold III, "Dimensional Stability of Low Expansivity Materials – Time dependent changes in optical contact interfaces and phase shifts on reflection from multi-layer dielectrics," Ph.D. dissertation, University of Arizona, Tucson, AZ, 1976.
31. F. Riehle, "Use of optical frequency standards for measurement of dimensional stability," *Meas. Sci. Technol.*, **9**, pp. 1042-1048, 1998.

32. V. G. Badami and S. R. Patterson, “A Frequency Domain Method for the Measurement of Nonlinearity in Heterodyne Interferometry,” *Precision Engineering*, Vol. 24, No. 1, pp. 41-49, 2000.
33. V. G. Badami and S. R. Patterson, “A Method for the Measurement of Nonlinearity in Heterodyne Interferometry,” *Proceedings of the 13th Annual Meeting of the American Society for Precision Engineering (ASPE)*, St. Louis, MO, pp. 530-533, 1998.
34. V. G. Badami and S. R. Patterson, “ Investigation of Nonlinearity in High Accuracy Heterodyne Interferometry,” *Proceedings of the 12th Annual Meeting of the American Society for Precision Engineering (ASPE)*, Norfolk, VA, pp. 153-156, 1997.
35. S. Patterson, and J. Beckwith, “Reduction of systematic errors in heterodyne interferometry,” *Proceedings of the 8th International Precision Engineering Seminar (IPES), Compiegne, France*, pp. 101-104.
36. C. Wu, J. Lawall, R. D. Deslattes, “Heterodyne interferometer with subatomic periodic nonlinearlity,” *Applied Optic*s, **38**(19), pp. 4089-4094, 1999.
37. J. Lawall, E. Kessler, “Michelson interferometry with 10 pm accuracy,” *Rev. Sci. Instrum.*, **71**(7), pp. 2669-2676, 2000.
38. J. Lawall, J. M. Pedulla and Y. Le Coq, “Ultrastable laser array at 633nm for real-time dimensional metrology,” *Rev. Sci. Instrum.*, **72**(7), pp. 2879-2888, 2001.